

## Porous Carbons

## Significant Effect of Pore Sizes on Energy Storage in Nanoporous Carbon Supercapacitors

Christine Young,<sup>[a, b, c]</sup> Jianjian Lin,<sup>[a, b]</sup> Jie Wang,<sup>[b, d]</sup> Bing Ding,<sup>[e]</sup> Xiaogang Zhang,<sup>[e]</sup> Saad M. Alshehri,<sup>[f]</sup> Tansir Ahamad,<sup>[f]</sup> Rahul R. Salunkhe,<sup>[b]</sup> Shahriar A. Hossain,<sup>[g]</sup> Junayet Hossain Khan,<sup>[g]</sup> Yusuke Ide,<sup>[b]</sup> Jeonghun Kim,<sup>[h]</sup> Joel Henzie,<sup>[b]</sup> Kevin C.-W. Wu,<sup>[d]</sup> Naoya Kobayashi,<sup>\*, [i]</sup> and Yusuke Yamauchi<sup>\*, [g, h, j]</sup>

**Abstract:** Mesoporous carbon can be synthesized with good control of surface area, pore-size distribution, and porous architecture. Although the relationship between porosity and supercapacitor performance is well known, there are no thorough reports that compare the performance of numerous types of carbon samples side by side. In this manuscript, we describe the performance of 13 porous carbon samples in supercapacitor devices. We suggest that there is a “critical

pore size” at which guest molecules can pass through the pores effectively. In this context, the specific surface area (SSA) and pore-size distribution (PSD) are used to show the point at which the pore size crosses the threshold of critical size. These measurements provide a guide for the development of new kinds of carbon materials for supercapacitor devices.

## Introduction

Electrochemical supercapacitors are useful in many applications because they can deliver energy at higher rates than batteries while maintaining their specific power. However, the relatively low specific energies of supercapacitor devices remain a challenge that must be overcome.<sup>[1]</sup> The specific energy is given by the formula shown in Equation (1), in which  $E$  is the specific energy,  $C$  is the specific capacitance ( $\text{F g}^{-1}$ ), and  $V$  is the operation window (V).

$$E = \frac{1}{2} CV^2 \quad (1)$$

$C$  is determined by the dielectric properties of the electrode material and reflects its ability to accommodate charge and obtain higher specific energy values. Enlarging  $V$  is also a common strategy to improve the specific energy, typically by using different electrolytes. The practical operating voltage of aqueous electrolytes is approximately 1.0–1.3 V, as  $\text{H}_2/\text{O}_2$  evolution reactions occur at around 1.23 V. In organic electrolyte,  $V$  can be expanded to approximately 2.5–2.8 V depending on the ion size of the electrolytes.<sup>[2]</sup>

The high electrical conductivity, high surface area, and low cost of porous carbon materials make them ideal electrodes in electrochemical supercapacitor devices. In general, porous

[a] C. Young, Dr. J. Lin  
Key Laboratory of Sensor Analysis of Tumor Marker  
Ministry of Education, College of Chemistry and Molecular Engineering  
Qingdao University of Science and Technology, Qingdao 266042 (P.R. China)

[b] C. Young, Dr. J. Lin, Dr. J. Wang, Dr. R. R. Salunkhe, Dr. Y. Ide, Dr. J. Henzie  
International Centre for Materials Nanoarchitectonics (MANA)  
National Institute for Materials Science (NIMS)  
1-1 Namiki, Tsukuba, Ibaraki 305-0044 (Japan)

[c] C. Young  
Faculty of Science and Engineering, Waseda University  
3-4-1 Okubo, Shinjuku, Tokyo 169-8555 (Japan)

[d] Dr. J. Wang, Prof. K. C.-W. Wu  
Department of Chemical Engineering  
National Taiwan University, No. 1, Sec. 4  
Roosevelt Road, Taipei 10617 (Taiwan)

[e] Dr. B. Ding, Prof. X. Zhang  
Key Laboratory of Materials and Technologies for Energy Conversion  
College of Materials Science & Engineering  
Nanjing University of Aeronautics and Astronautics  
Nanjing 210016 (P.R. China)


[f] S. M. Alshehri, T. Ahamad  
Department of Chemistry, College of Science  
King Saud University, Riyadh 11451 (Saudi Arabia)

[g] S. A. Hossain, J. H. Khan, Prof. Y. Yamauchi  
Australian Institute for Innovative Materials (AIIM)  
University of Wollongong, Squires Way, North Wollongong  
NSW 2500 (Australia)  
E-mail: yyamauchi@uq.edu.au

[h] Dr. J. Kim, Prof. Y. Yamauchi  
School of Chemical Engineering &  
Australian Institute for Bioengineering and Nanotechnology (AIBN)  
The University of Queensland, Brisbane, QLD 4072 (Australia)

[i] Dr. N. Kobayashi  
TOC Capacitor, 3-20-32 Tenryucho, Okayashi Nagano 394-0035 (Japan)  
E-mail: naoya.kobayashi@tocc.co.jp

[j] Prof. Y. Yamauchi  
Department of Plant & Environmental New Resources  
Kyung Hee University, 1732 Deogyong-daero  
Giheunggu, Yongin-si, Gyeonggi-do 446-701 (South Korea)

 Supporting information and the ORCID identification number(s) for the author(s) of this article can be found under:  
<https://doi.org/10.1002/chem.201705465>.

carbon materials are classified into three categories according to their pore size: macroporous ( $> 50$  nm), mesoporous (2–50 nm), and microporous ( $< 2$  nm) materials.<sup>[3]</sup> A higher porosity yields higher surface areas, providing one of the key characteristics for high-performance electrochemical supercapacitors. Therefore, it is logical to assume that porous materials with high surface areas will yield more active sites for adsorption/desorption reactions and ion/electron transport in electrochemical applications.<sup>[4,5]</sup> However, high-surface-area carbon electrodes tend to be more complex, and other factors play a role in determining the capacitance. For example, in some cases, micropores cannot bear the relatively high loading of electrolyte guest species that mesopores can accommodate. This can lead to internal strain and degradation of energy storage with repeated charge/discharge cycles.<sup>[3]</sup> As a result, mesoporous carbon architectures are suitable candidates for exploring supercapacitor performance with various kinds of electrolytes, and have been a fruitful area of research for decades.

Numerous methods exist for the synthesis of mesoporous carbon architectures. Strategies include the use of soft-template, hard-template, and template-free methods, biomass-derived carbons, architectures derived from reticular chemistry, and so on.<sup>[6,7]</sup> In the soft-templating approach, surfactant molecules and polymeric sources are co-assembled into ordered mesostructures.<sup>[8–10]</sup> Inorganic templates (e.g., silica, alumina) are used as hard templates for the fabrication of porous carbons.<sup>[8–10]</sup> Metal-organic frameworks (MOFs) and covalent organic frameworks (COFs) are highly ordered materials that can be decomposed into highly porous carbon materials.<sup>[11]</sup> Bio-

mass resources derived from the cellulose/lignin of plants and other agricultural wastes can also be converted into activated porous carbons that generate relatively low total impact on the environment during their lifecycle.<sup>[12–14]</sup>

Many decades of research have been devoted to explaining the relationship between porosity and supercapacitor performance.<sup>[15–18]</sup> Although various carbon materials have been tested, to our knowledge, there have been no systematic studies of a large number of porous carbon samples side by side. In this manuscript, we describe the properties of 13 porous carbon samples synthesized through various methods. We propose that there is a threshold of the pore size (so-called “critical pore size”,  $P$ ) at which guest molecules can pass through and effectively navigate the porous network. Through careful investigation of both the specific surface area (SSA) and pore-size distribution (PSD) of various samples, we demonstrate the point at which the pore size crosses the threshold of critical size. Our findings provide a simple and quick optimization method for the fabrication and development of new carbon materials for industrial applications.

## Results and Discussion

The preparation of the various porous carbon materials prior to characterization is described in detail in the Experimental Section. Initially, the surface morphology of the materials was investigated with a scanning electron microscope (SEM, Hitachi S-4800) at an accelerating voltage of 5 kV (Figure 1). Samples A–D were derived from biomass materials using various ap-

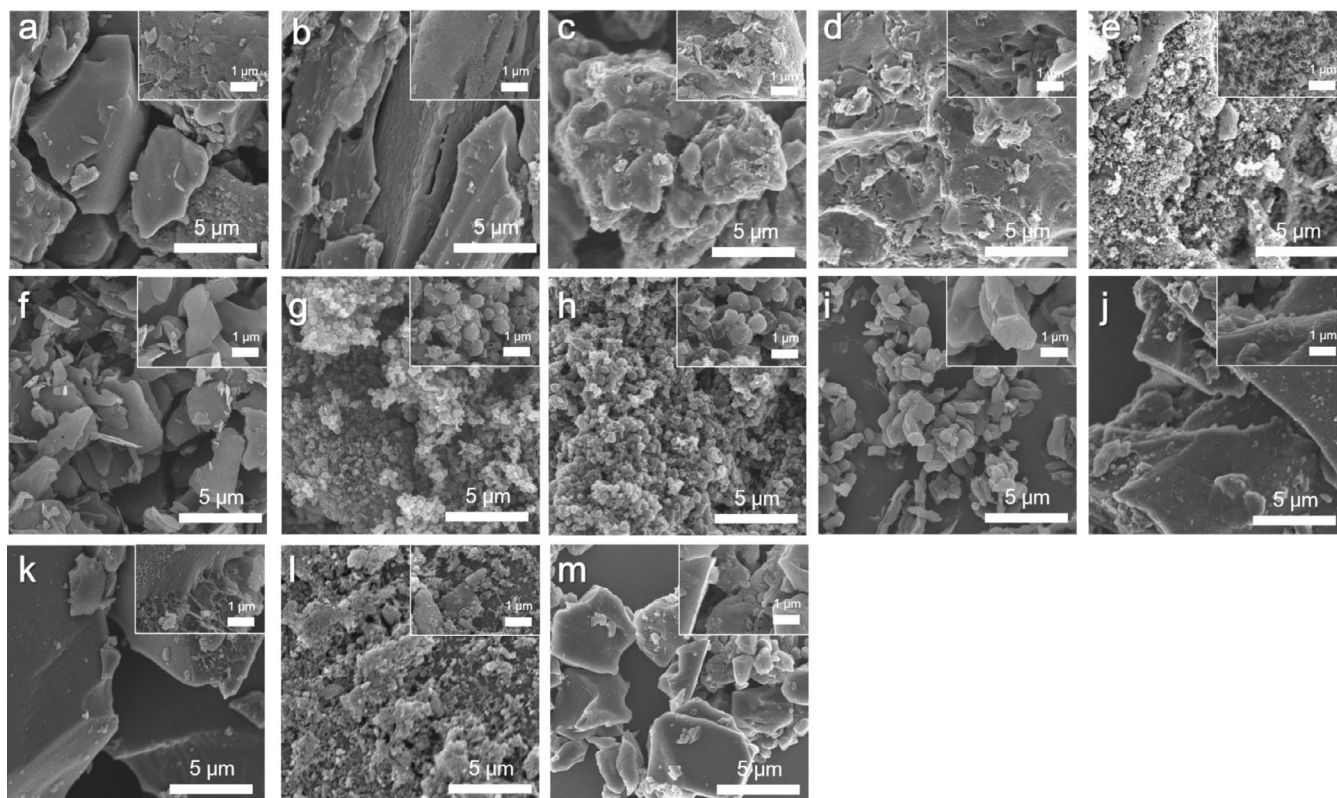


**Figure 1.** a–m) SEM images of Samples A–M, respectively.

proaches. Sample E was synthesized by using zinc layered hydroxide nitrate as a layered template.<sup>[19]</sup> Sample F was prepared from MXene.<sup>[20]</sup> Samples G and H were prepared from CaCO<sub>3</sub> precursors.<sup>[21]</sup> Samples I–M were synthesized through a soft-templating method by which the surface areas could be tuned according to the synthetic conditions.<sup>[22–25]</sup>

Nitrogen (N<sub>2</sub>) adsorption/desorption isotherms were collected for all materials to determine the porosity of the carbon samples (Autosorp operated at 77 K). The SSAs and PSDs were analyzed by density functional theory (DFT), and the details are summarized in Table 1. The isotherms and PSDs are shown in Figure 2. Samples A, C, and D possessed relatively high surface areas. However, whereas Sample A had an SSA of 1921 cm<sup>2</sup> g<sup>−1</sup>, its volume was composed of around 60.5% micropores. On the other hand, Samples C, D, F, H, I, L, and M were composed of <10% micropores, suggesting a high concentration of mesopores.

**Table 1.** Surface areas (*S*), pore volumes (*V*), micropore volumes (*V*<sub>micro</sub>), and percentages of micropores (*V*<sub>micro</sub>/*V*) for all prepared samples. *S* and *V* were calculated by the DFT method. *V*<sub>micro</sub> was calculated by the *t*-plot method. Note that micropores here are smaller than 2 nm.

Sample	<i>S</i> [m <sup>2</sup> g <sup>−1</sup> ]	<i>V</i> [cm <sup>3</sup> g <sup>−1</sup> ]	<i>V</i> <sub>micro</sub> [cm <sup>3</sup> g <sup>−1</sup> ]	<i>V</i> <sub>micro</sub> / <i>V</i> [%]
A	1921	1.2286	0.7430	60.5
B	463	0.2533	0.0611	24.1
C	2007	1.6050	0.1429	8.9
D	1858	1.6212	0.1216	7.5
E	328	0.2445	0.0298	12.2
F	704	0.6117	0.0387	6.3
G	685	0.4517	0.0822	18.2
H	1547	1.2930	0.0931	7.2
I	802	0.8453	0.0615	7.3
J	753	0.4488	0.0828	18.4
K	708	0.4610	0.0619	13.4
L	540	0.6870	0.0092	1.3
M	1479	1.5924	0.0432	2.7

In general, several factors affect the performance of supercapacitors, including surface area, pore size, material morphology/shape, conductivity, surface chemistry, and the ion size of the electrolytes.<sup>[26]</sup> In addition, carbon materials usually show the highest capacitances at lower current densities. Porous carbon materials can experience a decline in capacitance owing to insufficient charging time, which limits ion penetration through the pores of bulky particles.<sup>[27,28]</sup> To limit the influence of these various factors and focus on the influence of porosity, we performed our supercapacitor measurements at current densities of 0.4 mA cm<sup>−2</sup>. We used a coin-cell 2032-type supercapacitor device with a diameter of 20 mm and thickness of 3.2 mm. Both positive and negative electrodes were installed using the same active materials. A 10 mm diameter aluminum plate was used as the current collector. The electrode material consisted of 80 wt% active material, 15 wt% conductive agent, and 5 wt% PTFE. The electrolyte used was 2 M SBPBF<sub>4</sub> SL + DMS (9:1) solution. Galvanostatic charge/discharge curves of all carbon samples were measured. The first ten cycles were performed at the target current density of 0.4 mA cm<sup>−2</sup>, and

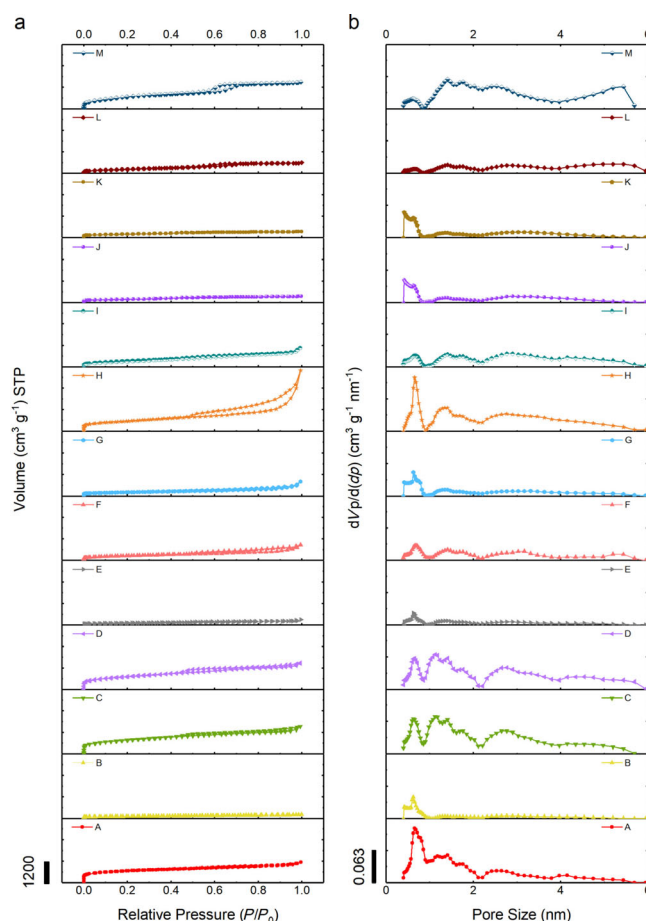


**Figure 2.** a) Nitrogen adsorption/desorption isotherms and b) pore-size distributions (PSDs) of all samples.

the tenth cycle was used for the calculation of capacity (see the Experimental Section).

All the discharge curves are linear in the whole discharge potential window, indicating nearly perfect capacitive behavior (Figure 3a). As shown in Figure 3, samples C, D, F, and M show relatively high capacities (>30 mA h g<sup>−1</sup>), which may be attributed to their high SSAs in addition to a high concentration of mesopores according to the PSDs (Figure 2b). Although Sample A had a high SSA compared with other samples, the capacity was only 18.31 mA h g<sup>−1</sup>, indicating that its high percentage of micropores negatively affects its performance. Overall, by comparing the capacities of these various carbon materials, we can see that the presence of mesopores is quite important.

It is reasonable to assume that pores larger than the size of the electrolyte ion and its solvation shell area are necessary to obtain a high capacitance. On the basis of the above results, we propose that there is a threshold of the pore size (so-called “critical pore size”, *P*) that can adequately enable the electrolyte ions to pass through all the pores. From the obtained N<sub>2</sub> adsorption isotherms, the distributions of cumulative surface area versus pore size were obtained (Figure S1, Supporting Information). To find the critical pore sizes, *P*, we define here the “effective-SSA” (E-SSA, i.e., the surface area contributed from larger pores than the selected pore sizes), as explained in Fig-



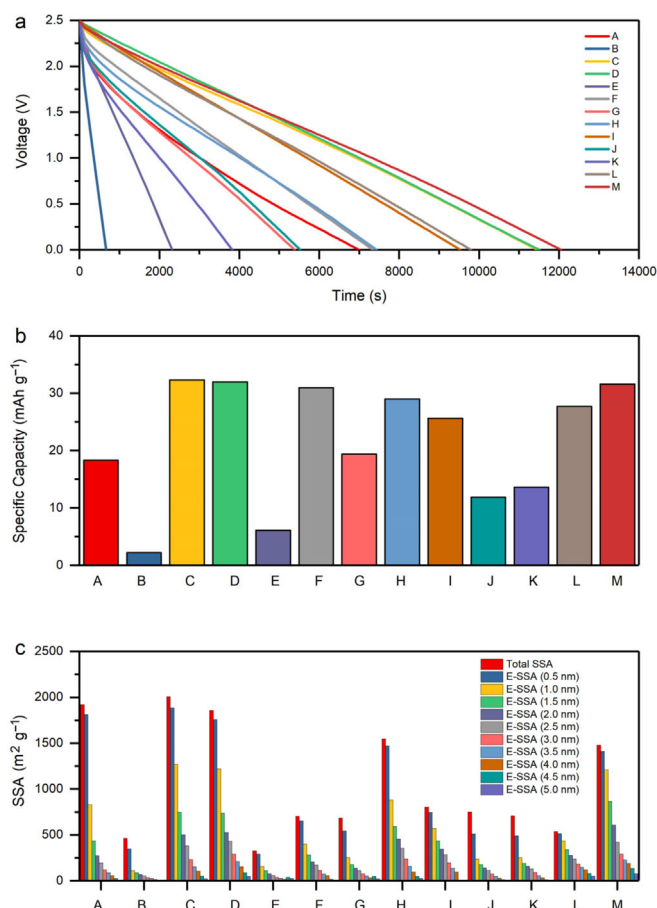


**Figure 3.** a) Galvanostatic charge/discharge curves of supercapacitors based on all the carbon samples in SBPBF<sub>4</sub> electrolyte, at a current density of 0.4 mA cm<sup>-2</sup>. b) Specific capacities of all carbon samples at 0.4 mA cm<sup>-2</sup>. c) Total SSA and E-SSA at particular pore sizes for all the carbon samples.

ure S2 (Supporting Information). To find the real critical pore size ( $P$ ), we calculated the E-SSAs by changing the selected pore sizes from 0.5 to 5 nm. It is known that the ionic radii of SBP<sup>+</sup> and BF<sub>4</sub><sup>-</sup> are 0.43 and 0.227 nm, respectively, so a minimum  $P$  value of 0.5 nm is reasonable if taking into account both the ion size and its solvent shell.<sup>[29,30]</sup> As an example calculation of the E-SSA, Sample A has an SSA of 1921 m<sup>2</sup> g<sup>-1</sup>, which results in E-SSA values of 1811 and 830 m<sup>2</sup> g<sup>-1</sup> for  $P$  values of 0.5 and 1.0 nm, respectively.

All the E-SSA values determined with different selected pore sizes are listed in Figure 3c. Figure 4 and Figure S3 (Supporting Information) display the relationship between the E-SSA and the specific capacity for all carbon samples by tuning the selected pore sizes. The coefficient of determination ( $R^2$ ) was calculated from the slope of the fitting line. The  $R^2$  values are quite low if the selected pore sizes are set to 0 nm. Higher values result in better  $R^2$  values, gradually increasing to 0.747 at  $P=3.0$  nm. At  $P>3.0$  nm the  $R^2$  values begin to decrease, probably because mesopores larger than 3 nm in diameter enable SBP<sup>+</sup> and BF<sub>4</sub><sup>-</sup> to pass through the pores easily. Note that the slope of the fitting line of  $P=3$  nm (Figure 3c) can be expressed as  $y=0.0996x+6.3345$ , in which  $x$  represents E-SSA and  $y$  represents specific capacity. If the E-SSA ( $x$ ) is zero, the

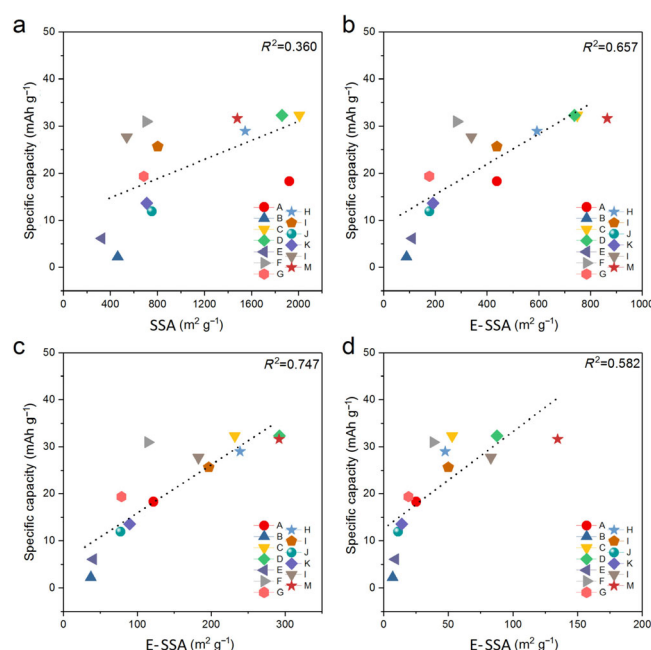


**Figure 4.** Relationship between specific capacity and effective surface area (E-SSA) using a) 0 nm, b) 1.5 nm, c) 3.0 nm, and d) 4.5 nm as the selected pore sizes.  $R^2$  is the coefficient of determination derived from the slope of the aggregate data.

capacity is 6.3345 mAh g<sup>-1</sup>. Thus, it seems reasonable that less capacity derives from pores smaller than 3 nm, although the mesopores dominate the performance.

## Conclusion

The performances of numerous porous carbon materials synthesized through various methods were tested in a supercapacitor device. We have demonstrated that there is a threshold of the pore size (critical pore size,  $P$ ) that can adequately enable the electrolyte ions to pass through all the pores. The highest-performing materials can be targeted by optimizing the pore sizes. This approach to the characterization of porous carbon materials could open a new path for the design of carbon materials for supercapacitors, as testing is a relatively quick process.

## Experimental Section

### Materials preparation

**Sample A (Coal tar-derived activated carbon):** Coal tar (1 g) was first pre-carbonized under a nitrogen atmosphere at 600 °C for 2 h to form chars. The sample was washed three times with acetone, ethanol, and water, and then ground together with KOH pellets (at a mass ratio of 1:1), put in a furnace under a nitrogen atmosphere, heated to 800 °C (ramp rate: 2 °C min<sup>-1</sup>), and held at that temperature for 2 h. The final sample was obtained by washing with HCl and water.

**Sample B (Jute-derived carbon #1):** Jute (1 g) was ground with a mortar and pestle into tiny fibrous pieces and then washed three separate times with acetone, ethanol, and water. The sample was

placed in a furnace under a nitrogen atmosphere, heated to 800 °C (ramp rate: 2 °C min<sup>-1</sup>), and held at that temperature for 2 h.

**Sample C (Jute-derived carbon #2):** Jute (1 g) was ground with a mortar and pestle into tiny fibrous pieces and then washed three separate times with acetone, ethanol, and water. The sample was placed in a furnace under nitrogen, heated to 800 °C (ramp rate: 2 °C min<sup>-1</sup>), and held at that temperature for 2 h. The sample was activated by grinding it together with KOH (1:1 mass ratio), after which it was heated to 700 °C (ramp rate: 2 °C min<sup>-1</sup>) and held at that temperature for 2 h. The final sample was washed with HCl and water prior to use.

**Sample D (Jute-derived carbon #3):** Jute (1 g) was ground with a mortar and pestle into tiny fibrous pieces and then washed three separate times with acetone, ethanol, and water. The sample was placed in a furnace under nitrogen, heated to 800 °C (ramp rate: 2 °C min<sup>-1</sup>), and held at that temperature for 2 h. Finally, the obtained carbon was activated by grinding it together with KOH (1:1 mass ratio) and then heating at 800 °C for 2 h. The final sample was washed with HCl and water prior to use.

**Sample E (Porous carbon nanosheets):** The preparation of this sample followed an existing method.<sup>[19]</sup> Zinc nitrate hexahydrate (11.9 g) was dissolved in distilled water (200 mL) and the pH was changed gradually to 7.0 with 0.5 M NaOH solution. The resulting precipitate was dried overnight. The precipitate (1 g) was suspended in 0.5 M gallic acid (250 mL) and then stirred vigorously for 2 h at room temperature (RT) under nitrogen. Next, the sample was heated (again under nitrogen) to 950 °C (ramp rate: 5 °C min<sup>-1</sup>) and held at that temperature for 2 h. The final sample was washed with HCl and water prior to use.

**Sample F (MXene-derived carbon):** According to a previous paper,<sup>[20]</sup> Ti<sub>3</sub>AlC<sub>2</sub> powder (2 g) was suspended in HF solution (25 mL; 40 wt%) at RT for 24 h. The resulting precipitate was washed thoroughly with deionized water to form the MXene, then dried under vacuum at RT for two days. The dried MXene was placed into a horizontal quartz tube furnace, which was then purged with argon and heated to 900 °C. Subsequently, it was exposed to dry chlorine gas for 2 h. After chlorination, the samples were held at 600 °C for 2 h under flowing ammonia gas to remove residual chlorine and chlorides trapped in the pores.

**Sample G (Porous carbon prepared from CaCO<sub>3</sub> #1):** According to a previous paper,<sup>[21]</sup> Na<sub>2</sub>CO<sub>3</sub> solution (0.33 M) and CaCl<sub>2</sub> solution (0.033 M) were dissolved in deionized water (100 mL). Dopamine hydrochloride was dissolved in tris(hydroxymethyl)aminomethane solution (10 mM) and the pH was adjusted to 8.5. This solution was stirred vigorously for 24 h. The sample was separated by centrifugation, and the resulting CaCO<sub>3</sub>-polydopamine composite was heated under nitrogen at 800 °C (ramp rate: 2 °C min<sup>-1</sup>) and held at that temperature for 2 h. The final sample was washed with HCl and water prior to use.

**Sample H (Porous carbon prepared from CaCO<sub>3</sub> #2):** The synthesis method was similar to that of Sample G except that the CaCO<sub>3</sub>-polydopamine composite was heated under nitrogen at 800 °C (ramp rate: 5 °C min<sup>-1</sup>) and held at that temperature for 2 h.

**Sample I (Hard-templated mesoporous carbon CMK-3):** The preparation of mesoporous carbon CMK-3 has been reported previously.<sup>[22]</sup> SBA-15 (1 g) was added to a mixture of sucrose (1.25 g) and H<sub>2</sub>SO<sub>4</sub> (0.14 g) dissolved in H<sub>2</sub>O (5 g). The mixture was placed in a drying oven for 6 h at 100 °C, and then for 6 h at 160 °C. The sample turned dark brown or black during the treatment in the oven. The silica powders containing partially polymerized and carbonized sucrose were treated again at 100 and 160 °C using the same drying technique after the addition of sucrose (0.8 g), H<sub>2</sub>SO<sub>4</sub>

(0.09 g) and H<sub>2</sub>O (5 g). Carbonization was completed by pyrolysis at 900 °C under vacuum. The carbon-silica composite obtained after pyrolysis was washed with HF solution to remove the silica template.

**Sample J (Soft-templated mesoporous carbon #1):** According to a previous paper,<sup>[23]</sup> phenol (0.61 g) was melted in a flask at 40–42 °C and mixed with NaOH aqueous solution (0.13 g; 20 wt%) under stirring. After 10 min, formalin (1.05 g; 37 wt% formaldehyde) was added dropwise and the sample was held below 50 °C. Upon further stirring for 1 h at 70–75 °C, the mixture was cooled to RT and the pH was adjusted to approximately 7.0 with HCl solution. The water was removed by vacuum evaporation below 50 °C, and the final product was dissolved in ethanol (20 wt% resol-ethanol solution). Pluronic F127 (0.5 g) was added to this resol-ethanol solution (5.0 g; 20 wt%). After stirring at RT for 10 min, the sample was dried under ambient conditions for 4 h; this was followed by thermal treatment at 120 °C for 24 h. The resulting samples were obtained after pyrolysis for 3 h at 350 °C (ramp rate: 1 °C min<sup>-1</sup>). Mesoporous carbon was obtained after carbonization under nitrogen at 800 °C (ramp rate: 1 °C min<sup>-1</sup>) and holding at that temperature for 2 h.

**Sample K (Soft-templated mesoporous carbon #2):** According to a previous paper,<sup>[24]</sup> the mesoporous carbon was prepared through a simple method using atom-transfer radical polymerization. Typically, the resol precursor (2.0 g, containing 0.25 g phenol and 0.15 g formaldehyde) was added to tetrahydrofuran (THF) solution (5.0 g, containing 0.1 g PEO<sub>125</sub>-*b*-PS<sub>230</sub> copolymer) and then stirred to form a homogeneous solution. The solution was poured into a dish to evaporate ethanol at RT in ≈5–8 h, then heated in an oven at 100 °C for 24 h. The product was removed from the dish and ground into a fine powder. The obtained sample was calcined at 800 °C for 3 h under nitrogen to obtain the mesoporous carbon.

**Sample L (Ordered mesoporous carbon prepared from carbon-silica nanocomposite #1):** According to a previous paper,<sup>[25]</sup> block copolymer F127 (1.6 g) was dissolved in ethanol (20.0 g, containing 1.0 g of 0.1 M HCl solution). The sample was stirred for 1 h at 40 °C to make a clear solution. Then, tetraethoxysilane (TEOS; 2.0 g) was dissolved in this solution. Next, resol-ethanol solution (5.0 g, 20 wt%) was added to the solution, which was then stirred for 1 h at RT. All three components of the sample were assembled during this one-step process. The assembled mixture was transferred to a dish and dried for 1 h at RT. After evaporation of the ethanol, thermal polymerization was conducted at 100 °C for 24 h in an oven. The resulting thin film was removed from the dish, carbonized under nitrogen at 350 °C (ramp rate: 1 °C min<sup>-1</sup>), and held at that temperature for 3 h, then at 800 °C (ramp rate: 5 °C min<sup>-1</sup>), holding at that temperature for 2 h. The resulting carbon-silica composites were immersed in HF solution (10 wt%) for 24 h to remove the silica, and then washed with water.

**Sample M (Ordered mesoporous carbon prepared from carbon-silica nanocomposite #2):** The synthetic approach was similar to that for Sample L. Block copolymer F127 (1.6 g) was dissolved in ethanol (8.0 g, containing 1.0 g of 0.2 M aqueous HCl). The sample was stirred for 1 h at 40 °C to make a clear solution. Next, TEOS (2.0 g) and resol-ethanol solution (5.0 g; 20 wt%) were added sequentially to the solution, which was then stirred for 2 h. The mixture was transferred to a dish and dried for 1 h at RT. After total evaporation of the ethanol, thermal polymerization was conducted at 100 °C for 24 h in an oven. The resulting thin film was removed from the dish and carbonized under nitrogen at 350 °C (ramp rate: 1 °C min<sup>-1</sup>), holding at that temperature for 3 h, then at 900 °C (ramp rate: 5 °C min<sup>-1</sup>), holding at that temperature for 2 h. The resulting carbon-silica nanocomposites were immersed in HF solu-

tion (10 wt%) for 24 h to remove the silica, and then washed with water.

### Electrochemical characterization

The electrochemical measurements were performed with a 2032-type coin-cell supercapacitor device. Both positive and negative electrodes were installed using the same active materials. A 10 mm diameter aluminum plate served as the current collector. The electrode material consisted of 80 wt% active material, 15 wt% conductive agent, and 5 wt% PTFE. SBPBF<sub>4</sub> (2 M) in SL/DMS (9:1 vol/vol) solution served as the electrolyte. Galvanostatic charge/discharge curves of all carbon samples were measured at a current density of 0.4 mA cm<sup>-2</sup> during the first ten cycles. The discharge curve of the tenth cycle was used to calculate the capacity using the formula  $C = I \times \Delta t / (m \times \Delta V)$ , in which  $C$  is the capacity (mAh g<sup>-1</sup>),  $I$  is the current (mA),  $\Delta t$  is the time (h),  $m$  is the mass (g) of the material contained in both electrodes, and  $\Delta V$  is the operating voltage (V).

### Acknowledgements

This work was partly supported by an Australian Research Council (ARC) Future Fellow (FT150100479), JSPS KAKENHI Grant Number 17H05393 (Coordination Asymmetry), Ministry of Science and Technology, Taiwan (106-2811-E-002-023), the Natural Science Foundation of the Higher Education Institutions of Jiangsu Province (16KJB430015), the National Natural Science Foundation (NNSF) of China (61604070), and the National Natural Science Foundation of Jiangsu Province (BK20161000). The authors extend their appreciation to the International Scientific Partnership Program (ISPP) at King Saud University (KSU) for funding this research work through ISPP-0097.

### Conflict of interest

The authors declare no conflict of interest.

**Keywords:** carbon • electrochemistry • mesoporous materials • nanoporous carbon • supercapacitors

- [1] L. Q. Mai, A. Minhas-Khan, X. C. Tian, K. M. Hercule, Y. L. Zhao, X. Lin, X. Xu, *Nat. Commun.* **2013**, *4*, 2923.
- [2] C. Zhong, Y. D. Deng, W. B. Hu, J. L. Qiao, L. Zhang, J. J. Zhang, *Chem. Soc. Rev.* **2015**, *44*, 7484–7539.

- [3] W. Li, J. Liu, D. Y. Zhao, *Nat. Rev. Mater.* **2016**, *1*, 16023.
- [4] Z. Y. Sui, Q. H. Meng, J. T. Li, J. H. Zhu, Y. Cui, B. H. Han, *J. Mater. Chem. A* **2014**, *2*, 9891–9898.
- [5] X. D. Huang, Y. F. Zhao, Z. M. Ao, G. X. Wang, *Sci. Rep.* **2014**, *4*, 7557.
- [6] X. Y. Lai, J. E. Halpert, D. Wang, *Energy Environ. Sci.* **2012**, *5*, 9944–9944.
- [7] Y. S. Hu, Y. G. Guo, W. Sigle, S. Hore, P. Balaya, J. Maier, *Nat. Mater.* **2006**, *5*, 713–717.
- [8] Y. Wan, D. Y. Zhao, *Chem. Rev.* **2007**, *107*, 2821–2860.
- [9] C. D. Liang, Z. J. Li, S. Dai, *Angew. Chem. Int. Ed.* **2008**, *47*, 3696–3717; *Angew. Chem.* **2008**, *120*, 3754–3776.
- [10] N. D. Petkovich, A. Stein, *Chem. Soc. Rev.* **2013**, *42*, 3721–3739.
- [11] R. R. Salunkhe, J. Tang, N. Kobayashi, J. Kim, Y. Ide, S. Tominaka, J. H. Kim, Y. Yamauchi, *Chem. Sci.* **2016**, *7*, 5704–5713.
- [12] Y. P. Zhai, Y. Q. Dou, D. Y. Zhao, P. F. Fulvio, R. T. Mayes, S. Dai, *Adv. Mater.* **2011**, *23*, 4828–4850.
- [13] X. L. Wu, T. Wen, H. L. Guo, S. B. Yang, X. K. Wang, A. W. Xu, *ACS Nano* **2013**, *7*, 3589–3597.
- [14] X. J. He, P. H. Ling, J. S. Qiu, M. X. Yu, X. Y. Zhang, C. Yu, M. D. Zheng, *J. Power Sources* **2013**, *240*, 109–113.
- [15] C. Largeot, C. Portet, J. Chmiola, P. L. Taberna, Y. Gogotsi, P. Simon, *J. Am. Chem. Soc.* **2008**, *130*, 2730–2731.
- [16] S. Kondrat, C. R. Perez, V. Presser, Y. Gogotsi, A. A. Kornyshev, *Energy Environ. Sci.* **2012**, *5*, 6474–6479.
- [17] J. Chmiola, G. Yushin, R. Dash, Y. Gogotsi, *J. Power Sources* **2006**, *158*, 765–772.
- [18] L. Zhang, X. Yang, F. Zhang, G. K. Long, T. F. Zhang, K. Leng, Y. W. Zhang, Y. Huang, Y. F. Ma, M. T. Zhang, Y. S. Chen, *J. Am. Chem. Soc.* **2013**, *135*, 5921–5929.
- [19] Y. Wang, H. Dou, B. Ding, J. Wang, Z. Chang, Y. L. Xu, X. D. Hao, *J. Mater. Chem. A* **2016**, *4*, 16879–16885.
- [20] B. Ding, J. Wang, Y. Wang, Z. Chang, G. Pang, H. Dou, X. G. Zhang, *Nano-scale* **2016**, *8*, 11136–11142.
- [21] S. Kim, C. B. Park, *Langmuir* **2010**, *26*, 14730–14736.
- [22] S. Jun, S. H. Joo, R. Ryoo, M. Kruk, M. Jaroniec, Z. Liu, T. Ohsuna, O. Terasaki, *J. Am. Chem. Soc.* **2000**, *122*, 10712–10713.
- [23] Y. Meng, D. Gu, F. Zhang, Y. Shi, L. Cheng, D. Feng, Z. Wu, Z. Chen, Y. Wan, A. Stein, D. Y. Zhao, *Chem. Mater.* **2006**, *18*, 4447.
- [24] Y. Deng, T. Yu, Y. Wan, S. Shi, Y. Meng, D. Gu, L. Zhang, Y. Huang, C. Liu, X. Wu, D. Zhao, *J. Am. Chem. Soc.* **2007**, *129*, 1690.
- [25] R. L. Liu, Y. F. Shi, Y. Wan, Y. Meng, F. Q. Zhang, D. Gu, Z. X. Chen, B. Tu, D. Y. Zhao, *J. Am. Chem. Soc.* **2006**, *128*, 11652–11662.
- [26] L. Wei, M. Sevilla, A. B. Fuertes, R. Mokaya, G. Yushin, *Adv. Energy Mater.* **2011**, *1*, 356–361.
- [27] W. Xing, S. Z. Qiao, R. G. Ding, F. Li, G. Q. Lu, Z. F. Yan, H. M. Cheng, *Carbon* **2006**, *44*, 216–224.
- [28] J. Chmiola, G. Yushin, Y. Gogotsi, C. Portet, P. Simon, P. L. Taberna, *Science* **2006**, *313*, 1760–1763.
- [29] M. Ue, *J. Electrochem. Soc.* **1994**, *141*, 3336–3342.
- [30] E. Perricone, M. Chamas, J. C. Lepretre, P. Judeinstein, P. Azais, E. Raymundo-Pinero, F. Beguin, F. Alloin, *J. Power Sources* **2013**, *239*, 217–224.

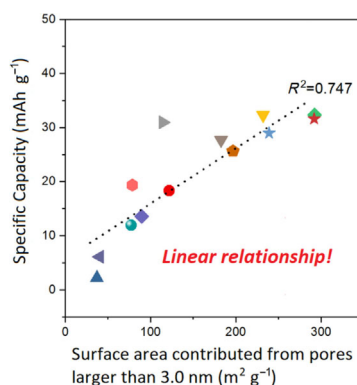
Manuscript received: November 17, 2017

Version of record online: ■■■ 0000

## FULL PAPER

**Designing supercapacitor materials:**

Several porous carbon samples were tested in supercapacitor devices. There is a “critical pore size” at which guest molecules can pass through the pores effectively. Measurements of specific surface area (SSA) and pore-size distribution (PSD) provide a guide for the development of new kinds of carbon materials for supercapacitor devices (see figure).

**Porous Carbons**

C. Young, J. Lin, J. Wang, B. Ding, X. Zhang, S. M. Alshehri, T. Ahamad, R. R. Salunkhe, S. A. Hossain, J. H. Khan, Y. Ide, J. Kim, J. Henzie, K. C.-W. Wu, N. Kobayashi,\* Y. Yamauchi\*



**Significant Effect of Pore Sizes on Energy Storage in Nanoporous Carbon Supercapacitors**

